

Gradient-free quantum optimization on NISQ devices

L. Franken^{1, 6}, B. Georgiev^{1, 6}, S. Muecke^{4, 6}, M. Wolter^{3, 5}, N. Piatkowski^{1, 6}, and C. Bauckhage^{1, 2, 6}

¹Fraunhofer Institute for Intelligent Analysis and Information Systems, 53757 Sankt Augustin, Germany

²Bonn-Aachen International Center for Information Technology (b-it), 53113 Bonn, Germany

³Fraunhofer Institute for Algorithms and Scientific Computing SCAI, 53757 Sankt Augustin, Germany

⁴Artificial Intelligence Group, TU Dortmund University, Germany

⁵Computer Science Department, University of Bonn, Germany

⁶Competence Center for Machine Learning Rhine-Ruhr (ML2R)

Abstract

Variational Quantum Eigensolvers (VQEs) have recently attracted considerable attention. Yet, in practice, they still suffer from the large quantum computational overhead in estimating cost function gradients for large parameter sets or resource-demanding reinforcement strategies. Here, we consider recent advances in weight-agnostic learning and propose a strategy that addresses the *trade-off between finding appropriate circuit architectures and parameter tuning*. We investigate the use of evolutionary algorithms which first spawn circuit's offspring and then evaluate them via genetic competition, thus circumventing some of the previous issues common parameter based approaches. We test our methods both via simulation and on real quantum hardware and use them to solve the transverse field Ising Hamiltonian and the Sherrington-Kirkpatrick spin model. We investigate which mutation operations most significantly contribute to the optimization. The resulting insights lay out a path for further refinement of gradient-free strategies. We test the algorithm's performance both in simulation and on real quantum hardware, finding only a minor slowdown in the case of real machines, particularly if the cost function is more non-local.

1 Introduction

The current era of Noisy-Intermediate Scale Quantum Computing (NISQ) [23] promises to deliver first instances where quantum computers outperform classical ones on useful tasks. Indeed, in late 2019 such quantum supremacy was first obtained by the *Sycamore* quantum processor [2]. However, the noise inherent to NISQ machines prevents the application of well-known quantum algorithms with proven speedups. Oppositely, Variational Quantum Eigensolvers (VQE) [18] are more robust and hence well suited to available hardware. In VQE one iteratively optimizes a set of parameters with respect to their performance in a given cost function. Applications include, among others, ground state approximation [3, 21], simulation of imaginary-time evolution [16] and quantum machine learning [7]. However, NISQ devices still suffer from limitations such as low circuit depth caused by large error probabilities and short decoherence times. Moreover, the recently exposed problem of barren plateaus [17] causes gradients of cost functions to become exceedingly small as the number of system qubits is increased. In turn, this diminishes some of VQE's potential for realistically sized problems [12]. To bypass such issues, evolutionary strategies have been proposed as an option to discover a set of rotation axes that more closely relates to the problem we are trying to optimize.

Our contribution In this paper we evaluate evolutionary approaches by testing methods closely related to the recent AdaptVQE ansatz [10]. The mutations of our so called QNEAT scheme feature insertion, deletion, swapping and modification of circuit gates. By testing the algorithm on Hamiltonians with varying difficulty, we show how the importance of these operations depends on the given problem. For instance, in case of a trivial local Hamiltonian, the algorithm chooses to mostly forgo usage of the latter three operations and instead mainly inserts gates. Oppositely, for a Spin-Glass Hamiltonian, the success rate of the swapping operation is highest, indicating

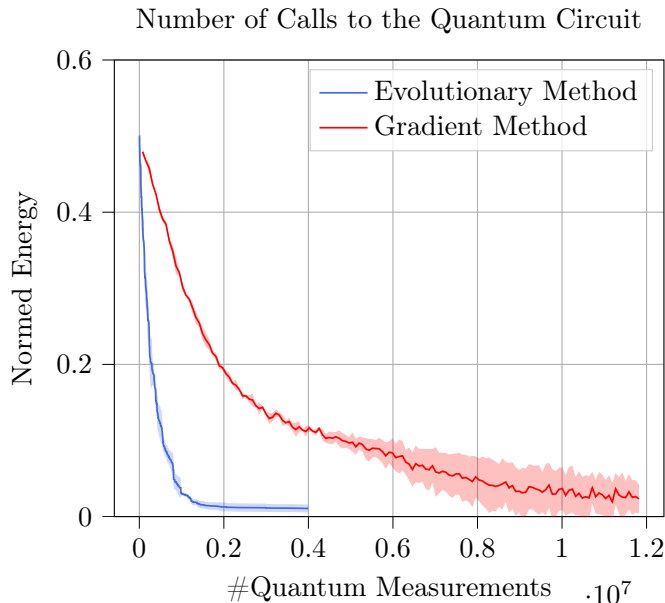


Figure 1: Optimization versus calls to the quantum circuit for an evolutionary and a gradient-based method. The system has eight qubits and minimizes a transverse-field Ising Hamiltonian. The evolutionary method creates four new circuits in every generation, keeping only the best-performing mutation. The gradient method determines derivatives using parameter shifts [4] and is conducted with learning rate $\eta = 0.1$, utilizing an ansatz with 150 parameters.

that for more difficult problems gate insertion might be insufficient for successful optimization. These results refine upon the observations of [32]. Also, we compare how the QNEAT scheme’s performance is reduced when run on real quantum hardware. Consistent with expectation, optimization towards ground states prepared by non-local gates suffers non-trivial slowdown when run on IBMQ machines *Manhattan*, *Toronto* and *Paris*. Finally, we compare the speed of convergence of the QNEAT scheme with gradient descent methods and find the evolutionary scheme to drastically outperform the gradient method (Fig. 1). However, we note that such performances are subject to a strong dependence on system size and the current literature still lacks the respective theoretical treatment. However, we are optimistic that evolutionary strategies retain comparable performance for larger systems.

Related Work Unfolding concurrently to variational approaches [10], work at the intersection of evolutionary- and quantum computing broadly falls into two categories: quantum-inspired evolutionary algorithms for classical computers and simulated quantum evolutionary algorithms.

Quantum-inspired evolutionary algorithms for classical computers simulate quantum bits, gates, superposition, and measurement to solve various problems within the usual standard framework [34]. In general, this line of work intends to benefit from a richer quantum representation. Simulated quantum-bits allow linear superposition of multiple states and are handled by synthetic quantum gates [34]. The concept is applicable to deep neural network architecture optimization where it produces effective yet simple convolutional networks [31]. However, computational costs of quantum simulations appear to be considerable. For instance, the authors of [31] report that 20 Nvidia K80 GPUs ($20 \cdot 24 = 480$ GB of GPU Ram) were required for two days.

Simulated quantum evolutionary algorithms seek to utilize evolutionary algorithms in a simulated quantum computation environment. Early work evolved a solution to Deutsch’s problem [28]. More recently, the Ising model of quantum computation was used to evolved multiple quantum gates in simulation [13]. Similarly [19] utilized qbit encoding and the Ising model to create quantum like behaviour on FPGA-Hardware.

Quantum evolutionary computing has long been held back by limited availability and access to of working quantum hardware [27, 14]. The related AdaptVQE approach [10] is gradient based. To the best of our knowledge this paper presents the first application of a NEAT-based evolutionary quantum algorithm on a real device.

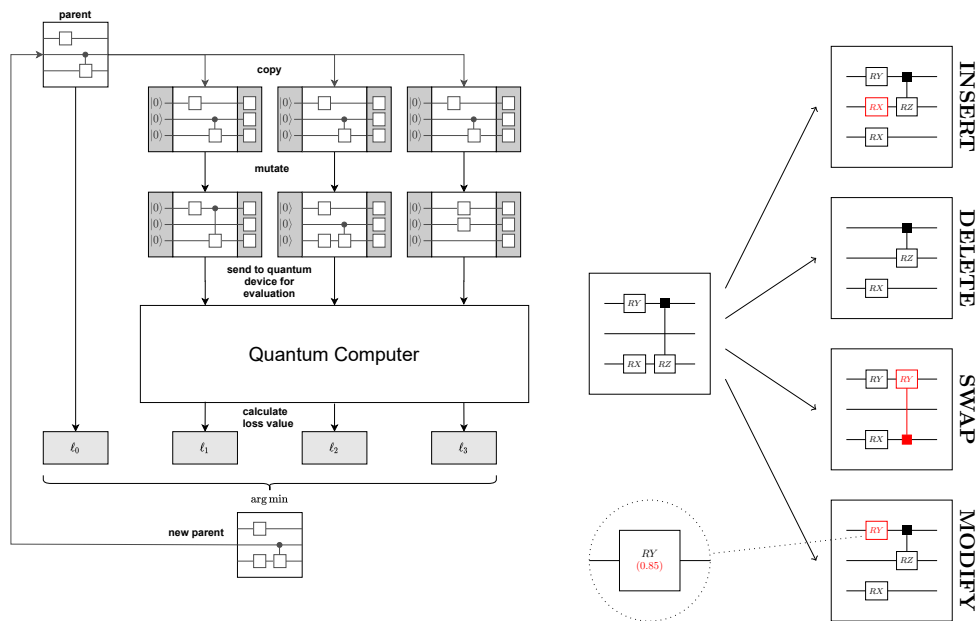


Figure 2: (Left) Outline of evolutionary circuit discovery: Starting with a random initial parent with known loss value, we create copies and mutate them using our custom mutation strategy using operations for instance as shown on the right. The offspring population is then evaluated on the quantum machine. The circuit with lowest loss value (the original parent included) becomes the parent circuit of the next generation. This procedure is repeated until an appropriate convergence criterion is satisfied. (Right) Mutation performs one of 4 actions with certain probabilities, we show these on the right. **INSERT:** Add random gate at random position; **DELETE:** Delete gate at random position; **SWAP:** Replace gate at random position with random new gate; **MODIFY:** Change parameter of gate at random position.

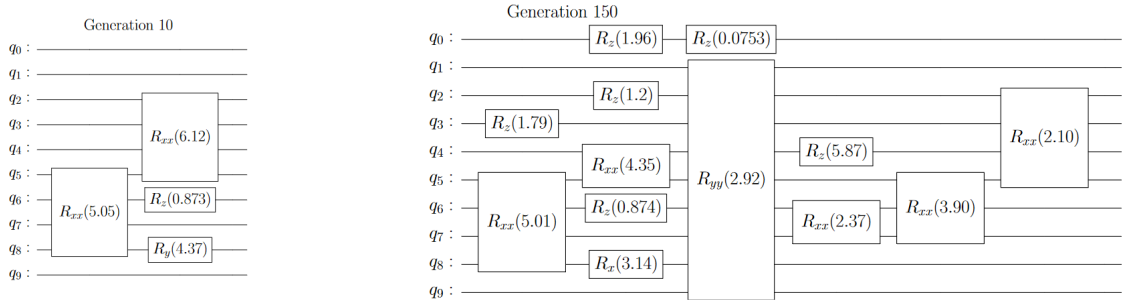


Figure 3: Circuit diagram of the gradual evolution of the circuit architecture optimization the transverse field Ising Hamiltonian, (*Left*) after 10 generations and (*Right*) after 150 generations. The notation R_i with $i \in \{x, y, z, xx, yy, zz\}$ represents a rotation gate wrt to axis i (for the purpose of clarity the explicit rotation’s angles are omitted). Note that gates spanning multiple qubits are only applied to the upper- and lowermost qubit. Note that by generation 150 some previously present gates with redundant parameters are removed. Moreover, the circuit generally reflects intelligence in its design and indeed is nicely aligned the expected useful set of gates for the TFI problem.

2 Augmenting Topologies through Evolution

In general, evolutionary algorithms (EA) [8, 9] iteratively work with a *population* of solution candidates, and optimization is carried out over a number of *generations*. In each generation, μ candidates that constitute the *parent* population produce an *offspring* population of λ candidates by means of crossover and *mutation*; these operations are specific to the problem domain at hand. In our application, candidates are quantum circuits, and mutations cause small changes to the circuit, such as addition or removal of a gate, or nudging of a gate’s parameter. The newly obtained offspring candidates are evaluated with respect to the loss function and sorted into the parent population, replacing parents with higher loss value. This *selection* step emulates natural selection in biology, where better adapted individuals survive. As the parent population is maintained during selection, the best individual that was ever observed since the first generation always survives. This property is known as *elitism* and ensures that the overall best loss value always monotonically decreases over time. The μ best candidates proceed to form the parent population of the next generation. If none of the offspring individuals yields an improvement, the original parent population carries over to the next generation unchanged. This EA scheme is known in literature as a $(\mu + \lambda)$ EA and is among the most representative and best-understood evolutionary optimization strategies [11, 6].

The classical Neuro-Evolution of Augmenting Topologies (NEAT) algorithm [29] adapts evolutionary algorithms for network structure and weight optimization. Evolution initially begins with a minimal structure to reduce the risk of evolving at an overly complex solution. Due to the competing identities [29] problem we choose to forego crossover. Our non-mating QNEAT algorithm evolves candidate solutions using a domain-specific mutation operator, which we describe in the upcoming section.

3 Algorithm Outline

In this Section we discuss the details of our proposed NEAT-like procedure, operating on quantum circuits instead of neural network graphs: in particular, we define the required set of gates and the building blocks of the architecture. The set of possible circuits \mathcal{U} should at least hypothetically be the entire unitary group over the chosen number of qubits. This feat is easily attainable by giving the algorithm access to a universal set of gates [20]. Using an evolutionary algorithm we attempt to find a circuit $U_c \in \mathcal{U}$, which performs best with respect to some cost function f . Every circuit U_c is a product of unitary matrices such that $U_c = \prod_i U_i$, each of which is defined by generator and a parameter pair (g_i, θ_i) , i.e.

$$U_i \equiv U(g_i, \theta_i) = \exp\left(-i \frac{\theta_i}{2} g_i\right). \quad (1)$$

In this notation g_i denotes an element of a set of Pauli-generators \mathcal{G} for experiments chosen to be

$$\mathcal{G} = \{\sigma_i^{(\mu)}, \sigma_i^{(\mu)} \sigma_j^{(\mu)}\} \quad (2)$$

with $\mu \in \{x, y, z\}$ and $i \neq j$ and $1 \leq i, j \leq n$.

For each circuit there is an associated value defined by the expectation with respect to some target Hamiltonian H , written in density matrix formulation with $|\psi_0\rangle$ as initial state:

$$f(U_c) \equiv \text{Tr} [H U_c |\psi_0\rangle\langle\psi_0| U_c^\dagger] \quad (3)$$

Finding a circuit U_{opt} which minimizes f is an optimization task over the search space \mathcal{U} . This space \mathcal{U} is defined through a mix of discrete and continuous values, namely generators g_i and qubit indices and parameters θ_i , respectively. While traditional gradient methods can optimize only the real-valued parameters θ_i on fixed circuit layouts, they cannot learn the overall circuit structure, because the existence or non-existence of a gate, for instance, is not differentiable.

However, evolutionary algorithms with elitist selection as described above can deal with non-differentiable and even non-continuous search spaces, because they only require some mutation operator \mathbf{m} that takes a circuit U_c as input, applies random changes to it, and thus produces a slightly different circuit \tilde{U}_c . More formally, $\mathbf{m}(U_c) = \tilde{U}_c$, where U_c is a random variable over \mathcal{U} . If U_c has support everywhere on \mathcal{U} , i.e. $P(U_c = U_{c'}) > 0$ for all $U_{c'} \in \mathcal{U}$, then the EA is guaranteed to converge to the global optimum [24].

Assuming $\mu = 1$, we have a single parent circuit $U^{(t)}$ in generation t . To find the parent of the following generation $t+1$, we sample λ instances of $\mathbf{m}(U^{(t)})$ and take their argmin with respect to f , including the parent $U^{(t)}$ itself:

$$U^{(t+1)} = \arg \min_{\tilde{U} \in \tilde{\mathcal{U}}} f(\tilde{U}), \quad \text{where} \quad (4)$$

$$\tilde{\mathcal{U}} = \{\tilde{U}_i \sim \mathbf{m}(U^{(t)}) : 1 \leq i \leq \lambda\} \cup \{U^{(t)}\}$$

This process may be repeated until no more changes occur, i.e. $f(U^{(t+\tau)}) = f(U^{(t)})$ for a fixed threshold $\tau > 0$, or some budget, such as a maximum number of computations on the quantum device, is depleted.

Note the distinct difference to the framework of regular VQE [18] where a circuit is defined by a set of gates U_i , each of which carry a respective parameter θ_i . Then, a gradient method is used to optimize

$$\theta_c = \arg \min_{\vec{\theta}} f(U(\vec{\theta})). \quad (5)$$

This is the setup in which we encounter the usual caveats outlined in Section 1.

Hence, the previous paragraph formalizes a combined evolution approach in the spirit of well established network architecture search methods NEAT [29] thereby conducting a search over circuit architectures that intrinsically correspond to problem. The macroscopic picture is shown in Fig. 2. Each generation consists of two steps. The specifics of the mutation strategy are individual specifically for the application and we postpone their discussion to the experimental section of this note.

Convergence The speed of convergence of this approach depends on the chosen problem. To shed some light on this issue we devise an upper and lower bounds for the number of generations required as well as for simple and complex ground state energy estimation.

Proposition 1. *Given a maximally local Hamiltonian*

$$H = \sum_{i=1}^n \sigma_i^{(z)} \quad (6)$$

in each random-gate-choice event the probability of drawing a useful gate is $\geq \frac{1}{4}$ and the number of generations required for optimization is of order $O(n)$.

Proposition 2. *Let $|\psi_0\rangle$ be the n -qubit ground state to a non-local Hamiltonian defined by*

$$|\psi_0\rangle = \sum_{x \in \{0,1\}^n} a_x |x\rangle \quad (7)$$

with 2^n independent amplitudes a_x . Our algorithm requires $O(2^n)$ operations to find $|\psi_0\rangle$.

Please find the respective proofs in Appendix A. With these loose lower and upper bounds we establish a spectrum in which reasonable complexity estimations can be made. We argue, considering the physics involved in typical quantum simulation the length of the required gate sequence does not suffer from the problem stated in Proposition 2. Consider a generic Hamiltonian mapped to qubits

$$H = \sum_{i=1}^r \prod_{j=1}^{r_i} \sigma_{q_j}^j, \quad (8)$$

where $\sigma_{q_j}^j \in \{\sigma^{(x)}, \sigma^{(y)}, \sigma^{(z)}\}$, q_j is a qubit index, r is the number of Hamiltonian summands and r_i is the number of Paulis in one summand. We remind ourselves of the results in [5] (see Appendix A, Prop 2) and find the ground state of a product of r_j Paulis is prepared with $O(2^{r_j-1})$ operations. Let us relate r_j to problems our algorithm is addressing. In practical chemistry simulations we are mostly concerned with electronic Coulomb interaction. For example the potential between states k and ℓ is captured in second quantization by the term

$$V = V_{k\ell} a_k^\dagger a_k a_\ell^\dagger a_\ell, \quad (9)$$

where a_k^\dagger, a_k are creation and annihilation operators of state k . Commonly, the Bravyi-Kitaev transformation [25] is employed to map between fermionic physics formulated in second quantization and their qubit representation by Pauli operators. In this transformation r_i is upper bounded by 4, such that we can generally assume $r_i \in \mathcal{O}(\log n)$ and can thereby circumvent the exponential runtime imposed by Proposition 2.

4 Experimental Evaluation

We evaluate the performance of the QNEAT algorithm on standard VQE problems both in simulations and on real devices. For that purpose, we briefly summarize the set of considered operation during mutation and outline our numerical approach. We then describe physical systems with increasing difficulty on which we will run the experiments to estimate the algorithm’s general capabilities.

4.1 Implementation and Method

We use the publicly available quantum computing library *qiskit* [1] to define and modify quantum circuits in Python. This library is also capable of simulating quantum computing, both by calculating amplitudes analytically and by simulating shots.

We use a custom EA implementation to perform a (1+4)-EA using a special multi-level mutation strategy, which we explain in the following paragraph. The optimization run starts with a minimal random circuit, consisting of only a single gate with a uniformly sampled parameter. From this initial parent circuit we make 4 copies and mutate them independently using our mutation strategy, which yields the offspring population. The offspring circuits are sent to the IBM Q backend via *qiskit*’s API. From the measurement results we derive a loss value, which we explain in detail in another paragraph further down this section. The entire population is then sorted by loss value, and the circuit with lowest loss becomes the new parent circuit for the next generation. This process is repeated for 150 generations, during which the parent’s loss value monotonically decreases, approaching the global optimum.

Mutation strategy The mutation strategy consists of a two-level random process. In a first step, we choose an action from a list of options. Then, we sample parameters for the chosen action and apply the changes directly to the circuit object. Possible actions (with their respective occurrence probabilities in parentheses) are:

- **INSERT** (50%): Sample generator g and parameter θ uniformly and insert the corresponding gate at a random position.
- **DELETE** (10%): Delete gate at a random position from the circuit.
- **SWAP** (10%): Combination of DELETE and INSERT at the same randomly chosen position.

- **MODIFY** (30%): Modify parameter of randomly chosen gate according to $\theta \mapsto \theta + \epsilon$ with $\epsilon \sim \mathcal{N}(0, 0.1)$.

See also Fig. 2 for some visual examples.

With a probability of 0.1, we repeat this entire mutation process after each action, leading to an expected number of $10/9 = 1.\bar{1}$ actions per mutation, the probability for 2 actions being about 9%, for 3 actions about 0.9% and for k actions $0.1^{k-1} \cdot 0.9$ in general. This scheme enables the mutation to perform arbitrarily large jumps in search space, as the probability to mutate from any circuit to any other circuit is strictly positive (provided it is made up of the same set of gates). This is easy to see considering the mutation operator could just delete all gates and then insert the gates constituting the optimal circuit one after the other. Even though this particular mutation is highly unlikely, the probability is non-zero, thus fulfilling the requirement of strictly positive support on all circuits in \mathcal{U} .

Evaluation To evaluate a circuit, we wrap it in multiple layers of static circuits. During the measurement process we append rotation layers to the circuit in accordance of the bases required by the Hamiltonian terms. Moreover, for all experiments we initialize the circuit with states that are neutral with respect to the optimization of a particular Hamiltonian. For instance, the initial state of an optimization task for a Hamiltonian with x - and z -terms is chosen to be the y -axis. Hence, initial energies are the exact mean between maximal and minimal eigenenergy.

For the purpose of consistency we leave most of the algorithm’s hyperparameters, like population size and mutation action probabilities, unchanged for the majority of experiments. The experiments are conducted for system sizes of 10 qubits.

In every generation, we collect thorough evolution data in order to extract information such loss value development over all generations, and types of mutations that lead to improvements. This information is valuable for further analysis and improvement of the procedure.

4.2 Considered Hamiltonians

The difficulty to find the minimal eigenvalue to a Hamiltonian is intimately tied to the entanglement of its ground state. Intuitively, the more entanglement required the more intricate the optimization landscape is. Therefore, we are first interested in our algorithms capability to perform in these non-convex circumstances. Secondly, entangling qubits requires multi-qubit gates which are on real hardware much more error-prone than locally acting ones. This should be reflected in differences in performance between experiments on a simulator versus on a real quantum machine. To gradually raise difficulty we transition in three steps from a maximally local problem to a spin-glass model only consisting of non-local terms. This gives us a chance test *a)* our algorithms capability to optimize increasingly difficult problems and *b)* the performance penalty obtained by running the algorithm on real machines. Let us shortly introduce the studied Hamiltonians.

Local Hamiltonian As a sanity check we first used a local problem

$$H = \sum_{i=1}^n \sigma_i^{(x)}. \quad (10)$$

Here $\sigma_i^{(x)}$ is the x -Pauli matrix acting on qubit i . Clearly, the ground state to this Hamiltonian is given by the n qubit product state $|\psi_0\rangle = |-\rangle_1 \otimes |-\rangle_2 \otimes \dots \otimes |-\rangle_n$. We expect that our algorithm not only finds the ground states consistently, but also that the performance is reliably reproduced by a real quantum machine.

Transverse Field Ising Model We next considered performance for the 1d spin-chain with correlation in the z -component and a transverse magnetic field with x -axis orientation [22]. Hence we get the Hamiltonian

$$H = -J \sum_{\langle i,j \rangle} \sigma_i^{(z)} \sigma_j^{(z)} - h \sum_{i=1}^n \sigma_i^{(x)}, \quad (11)$$

We only consider the ordered phase and get (anti-) ferromagnetic behavior for ($J > 0$) $J < 0$. For our purposes, we chose $J, h = 1$, i.e. opting for the anti-ferromagnetic behavior. Note that for Hamiltonian (11) the entanglement is superimposed to the previous local problem, posing the question which part of the optimization the algorithm conducts first. Our performance analysis also contains histograms of gates used successfully during the optimization, giving us insights into the algorithms priorities. Furthermore, the TFI is well-known to exhibit local minima, causing purely gradient based methods to fail ([33]). Our algorithms capability to navigate such landscapes is intuitively dependent on the distance traversed by each generation in Hilbert space. For our settings of hyperparameters, the vanishing of the energy landscape slope should not prohibit global optimization.

Sherrington-Kirkpatrick model The SK model simulates the behaviour of a frustrated spin glass [26] and was previously used as a benchmark model in quantum computing experiments [30], [3]. The model is given by the Hamiltonian

$$H = \sum_{i < j} J_{ij} \sigma_i^{(z)} \sigma_j^{(z)}, \quad (12)$$

where J_{ij} are randomly assigned couplings with $J_{ij} \in \{-1, 1\}$. For every run we constructed a randomly sampled instance of the SK model. However, the ground state energy of spin glass model instances is subject to concentration, hence properties such as optimization difficulty and ground state entanglement can be expected to behave consistently [15]. Note that such a Hamiltonian consists exclusively of correlation terms, which is why we expect this optimization problem to constitute a considerably harder problem than the previous experiments.

4.3 Experiments

All models were tested for 10 qubits on both simulation software provided by the *qiskit* library and actual quantum hardware *IBMQ Manhattan, Toronto* and *Paris*. Here, the respective left-hand plot exhibits the comparison between runs on real machines and simulation and the right-hand shows the same simulation runs in later generations. The runs are represented in energy versus generation where in each figure we show mean and variance of multiple runs. Additionally, to gain more insight into the actual behavior we also obtained histograms indicating which gates and evolutionary operations contributed to the optimization process.

Overall, we find our algorithm to perform well on all posed problems dealing both with entanglement requirements and local minima. The histograms indicate intelligent circuit design both in gate and operation choice and mostly confirms initial intuitions about which rotations are useful for certain tasks. We also observe a slight reduction in performance on quantum hardware as soon as multi-qubit gates are required for optimization.

Results The results for the local problem are depicted in Fig. 5. In this experiment we optimize a trivial sum of local σ_x Paulis over the full set of qubits. Clearly, the ground state then is given by the n qubit product state $|\psi_0\rangle = |-\rangle_1 \otimes |-\rangle_2 \otimes \dots \otimes |-\rangle_n$ which can be prepared by local operations. Since the problem lacks a correlation requirement between the qubits we expect fast convergence for both the simulation and the real runs and observe so in Fig. 5 with all runs rapidly converging to the global minimum. For both evaluated quantum machines the performance of the local Hamiltonian is very close between simulation and real machine. This result is consistent with expectation that optimization with rather noise-resilient local operations should be easily reproducible on quantum hardware. Fig. 4 shows the distribution over gates that contribute to the optimization. Since for this experiment we chose the y -eigenstate on all qubits as the initial state, we expect rotations around the z -axis (in the plot denoted 'rz') to be particularly useful. This intuition is confirmed and we find that by a large margin this is indeed the rotation chosen most frequently. Furthermore, the figure shows that slight alterations to the chosen z -rotations or replacements in favor of z -rotations are preferred over gate deletion. Thereby, the algorithm admits to a gradient-like functionality once the appropriate set of gates is found.

We next considered performance for the transverse-field Ising model (Fig 6). The simulated runs show reliable convergence even for a low small number of offspring created per generation. Note that for TFI the optimization of the local problem is bounded by the number of qubits in the

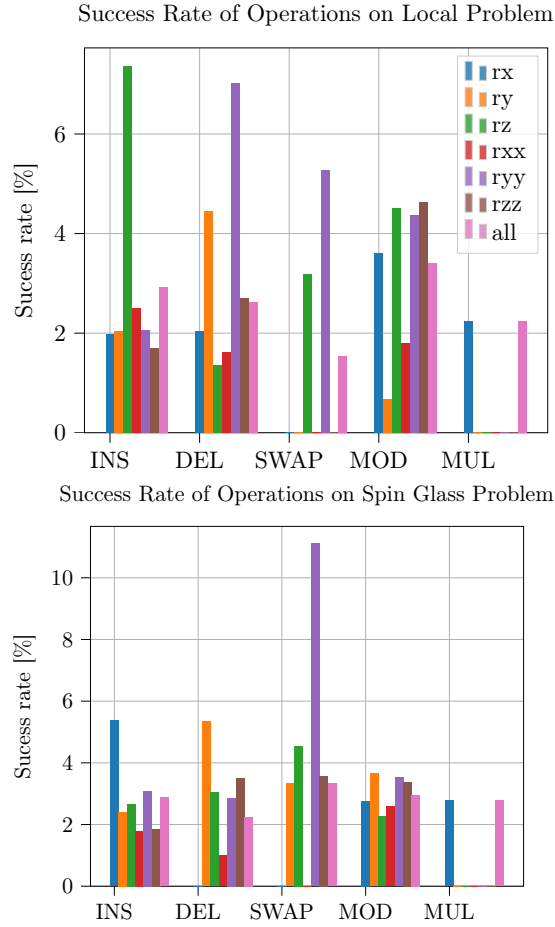


Figure 4: Success rate of various mutation operations for the gates available to the circuit on (Left) the maximally local problem and (Right) the SK Hamiltonian. Each plot refers to a mean over all runs conducted with respect to that Hamiltonian (3 on each real quantum device). The operations on the x -axis are from left to right *insert*, *delete*, *swap*, *modify*, *multiple*. We find all operations to provide a non-negligible number of useful additions to the optimization. Moreover, we observe distinct differences in the operations used between the Hamiltonians, where the trivial local problem exhibits a preference for gate insertion and the spin-glass problem for gate swapping.

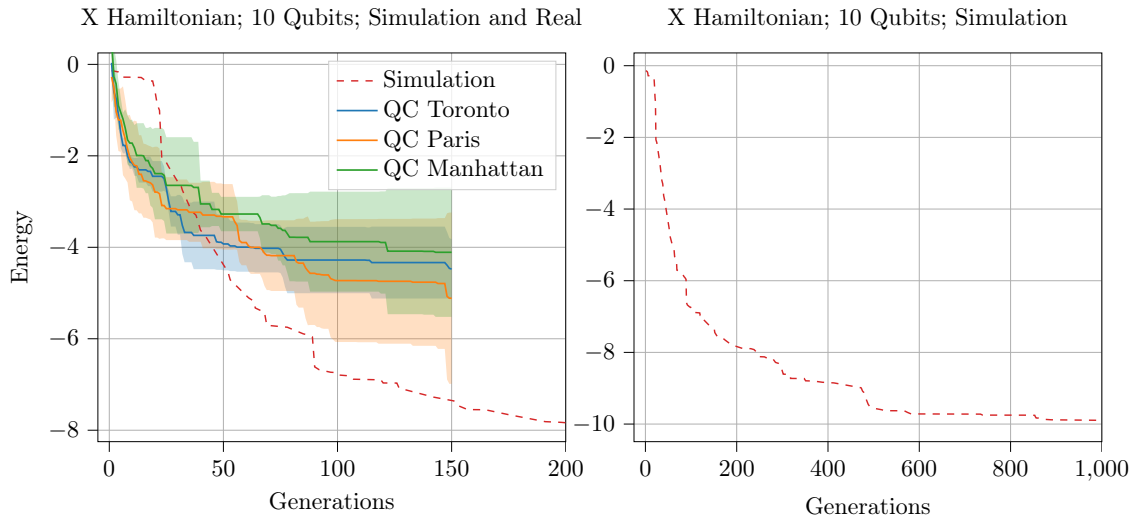


Figure 5: Performance of the QNEAT algorithm on real quantum computers *IBMQ Toronto*, *Paris* and *Manhattan* versus simulation for the maximally local problem on 10 qubits. All runs are shown as a mean of multiple runs with run length being limited by hardware availability. The exhibited performance is approximately similar between simulation and hardware with minor slowdown for the latter.

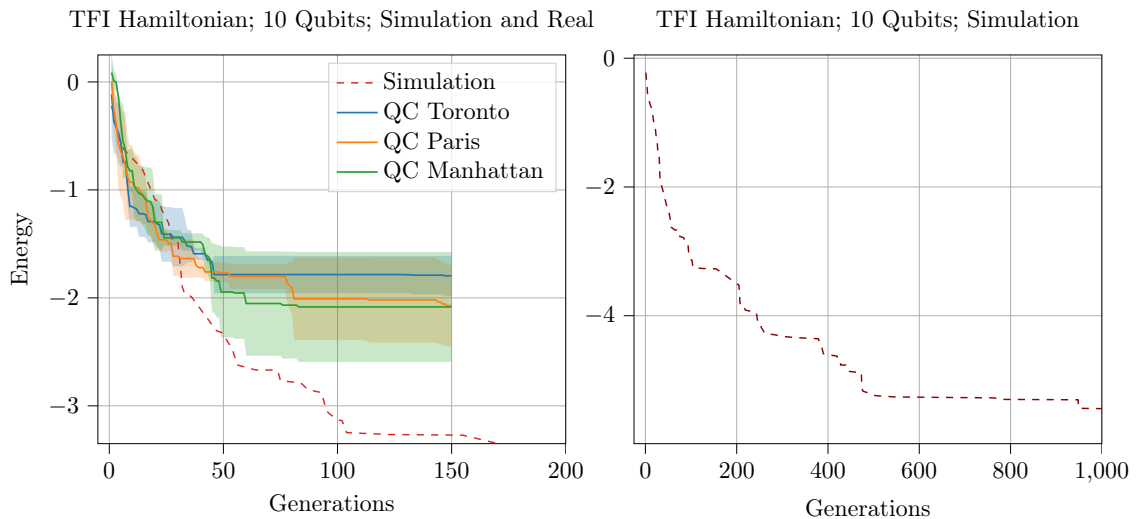


Figure 6: Performance of the QNEAT algorithm on real quantum computers *IBMQ Toronto*, *Paris* and *Manhattan* versus simulation for the transverse field Ising model on 10 qubits. The initial phases of the algorithm show larger similarity between simulation and real hardware compared to the optimization after generation 50. All runs are shown as a mean of multiple runs. For the optimization phase exhibited performance was approximately similar.

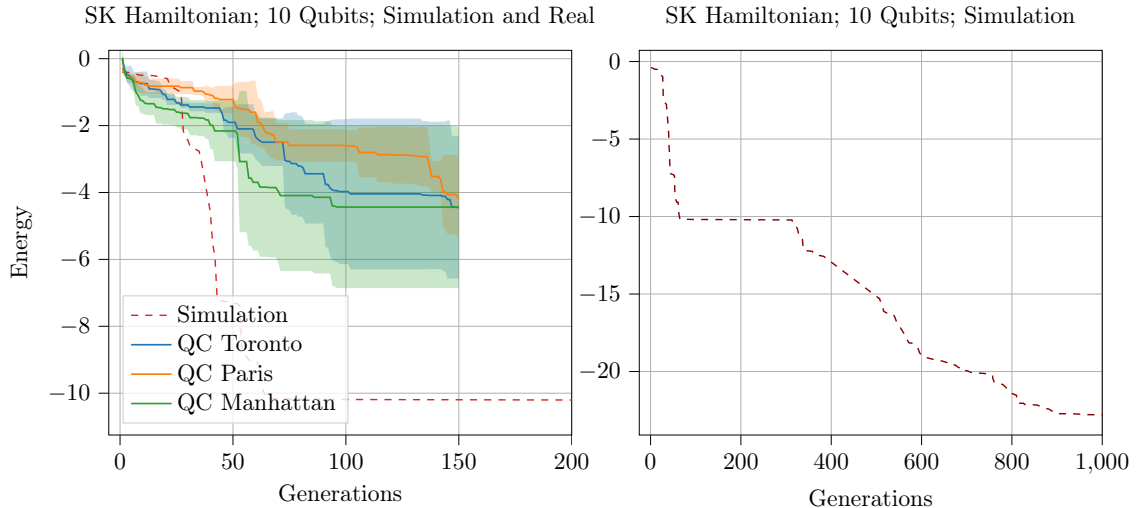


Figure 7: Performance of the QNEAT algorithm on real quantum computers *IBMQ Toronto*, *Paris* and *Manhattan* versus simulation for the Sherrington-Kirkpatrick Hamiltonian on 10 qubits. All runs are shown as a mean of multiple runs where vertical lines indicate the ending of a run. Note that run length was limited by hardware availability. Simulation runs show reliable optimization with the runs on real hardware lagging behind by a substantial margin. In comparison to the TFI case, this slowdown is observable from the beginning to the run and not only after 50 generations.

system, hence where this threshold is surpassed, the algorithm optimizes also with respect to the entangling gates. The right hand side clearly shows the desired behavior. In the real hardware case, during initial parts of the algorithm we consistently observe optimization similar to the simulation, yet notice a reduction in progress after ~ 50 generations. This might be caused by single-qubit gates losing their effectiveness after the initial stages of optimization.

Finally, the results of optimization of the SK model are shown in Fig. 7. In all cases the early generations exhibit reliable optimization and show strong capability to navigate entangled Hilbert space. However, the model’s particular proneness to local minima is exhibit by longer optimization stretches without progress. These stretches are present particularly often in the simulation case and we observe more stable optimization for the real hardware case. Unfortunately, the requirements on number of generations appears to be undercut quite substantially by the number of generations we were able to perform. However, Fig. 4 gives some insight into the algorithms gate and operation preferences during SK Hamiltonian optimization, exhibiting distinct differences to the previously discussed optimization of the local problem. We find the algorithm to be much more ‘cautious’ in adding gates to the circuit and rather requires all gate choices to be finely tuned as can be seen from the relatively low frequency of gate insertions in comparison to gate swapping. For this problem we start with local $\sigma^{(x)}$ -eigenstates in all qubits making the $\sigma_i^{(y)}\sigma_j^{(y)}$ particularly useful. Interestingly, such gates are predominantly added to the circuit via swapping and not via regular insertion. If this behaviour is connected to the unusual Hilbert space traversal conducted by evolutionary algorithms in general and the swapping operation in particular remains a question for further investigations.

5 Discussion

We proposed an algorithm to alleviate issues common to Variational Quantum Computing. Our approach minimizes number of gates in the circuit by discovering an architecture that corresponds to the posed problem via an evolutionary strategy. During an iterative process we create a set of mutations and subsequently conduct a tournament to determine the best performing candidates as parents for the next generation. We tested our algorithm on a set of Hamiltonians both as simulations and on real quantum hardware. On all posed problems the algorithm reliably finds circuits well suited for optimization with slight worsening for experiments on real quantum devices.

Moreover, the algorithm admits to the following expected properties.

Non-locality impedes optimization and as such convergence on more local problems proceeds faster. Between our experiments with exclusively local terms and the spin-glass model with only ZZ correlation terms this increase in hardness is reflected in our experimental results. However, in all cases the optimization yields solid results. Furthermore, the increased number Hamiltonian correlation terms implies the requirement for more multi-qubit gates during the ground state preparation. The vulnerability of such gates to noise can be observed in our experiments in a deceleration of runs on real hardware relative to the ones simulated. Our statistics indicate that the circuit design is indeed intelligent, meaning not only are useful gates visibly preferred but also are redundant gates removed over the course of the optimization. In comparison to gradient methods, this gradual circuit simplification yields the most pronounced advantage over other VQE methods.

Comparisons to related work show that few approaches utilize the full breadth of evolution strategies discovered as useful in the computer science literature. We show that all mutation operations *insertion*, *deletion*, *swapping* and *modification* has approximately equivalent success rates i.e. rates at which the operations provides a useful alteration to the circuit. This emphasizes that evolutionary strategies, applied to quantum optimization, is most effective with the full spectrum of operations available to the algorithm.

Acknowledgements

This work was supported by the Fraunhofer Cluster of Excellence Cognitive Internet Technologies (CCIT) and the Competence Center for Machine Learning Rhine-Ruhr (ML2R). ML2R is funded by the Federal Ministry of Education and Research of Germany (BMBF) (grant no. 01IS18038B).

References

- [1] Aleksandrowicz, G., Alexander, T., Barkoutsos, P., Bello, L., Ben-Haim, Y., Bucher, D., Cabrera-Hernández, F., Carballo-Franquis, J., Chen, A., Chen, C., et al.: Qiskit: An open-source framework for quantum computing. Accessed on: Mar **16** (2019)
- [2] Arute, F., Arya, K., Babbush, R., Bacon, D., Bardin, J.C., Barends, R., Biswas, R., Boixo, S., Brandao, F.G., Buell, D.A., Burkett, B., Chen, Y., Chen, Z., Chiaro, B., Collins, R., Courtney, W., Dunsworth, A., Farhi, E., Foxen, B., Fowler, A., Gidney, C., Giustina, M., Graff, R., Guerin, K., Habegger, S., Harrigan, M.P., Hartmann, M.J., Ho, A., Hoffmann, M., Huang, T., Humble, T.S., Isakov, S.V., Jeffrey, E., Jiang, Z., Kafri, D., Kechedzhi, K., Kelly, J., Klimov, P.V., Knysh, S., Korotkov, A., Kostritsa, F., Landhuis, D., Lindmark, M., Lucero, E., Lyakh, D., Mandrà, S., McClean, J.R., McEwen, M., Megrant, A., Mi, X., Michielsen, K., Mohseni, M., Mutus, J., Naaman, O., Neeley, M., Neill, C., Niu, M.Y., Ostby, E., Petukhov, A., Platt, J.C., Quintana, C., Rieffel, E.G., Roushan, P., Rubin, N.C., Sank, D., Satzinger, K.J., Smelyanskiy, V., Sung, K.J., Trevithick, M.D., Vainsencher, A., Villalonga, B., White, T., Yao, Z.J., Yeh, P., Zalcman, A., Neven, H., Martinis, J.M.: Quantum supremacy using a programmable superconducting processor. *Nature* (2019). DOI 10.1038/s41586-019-1666-5
- [3] Arute, F., Arya, K., Babbush, R., Bacon, D., Bardin, J.C., Barends, R., Boixo, S., Broughton, M., Buckley, B.B., Buell, D.A., et al.: Hartree-fock on a superconducting qubit quantum computer. arXiv preprint arXiv:2004.04174 (2020)
- [4] Banchi, L., Crooks, G.E.: Measuring analytic gradients of general quantum evolution with the stochastic parameter shift rule. *Quantum* **5**, 386 (2021)
- [5] Barenco, A., Bennett, C.H., Cleve, R., DiVincenzo, D.P., Margolus, N., Shor, P., Sleator, T., Smolin, J.A., Weinfurter, H.: Elementary gates for quantum computation. *Physical review A* **52**(5), 3457 (1995)
- [6] Droste, S., Jansen, T., Wegener, I.: On the analysis of the (1+ 1) evolutionary algorithm. *Theoretical Computer Science* **276**(1-2), 51–81 (2002)

- [7] Farhi, E., Neven, H.: Classification with quantum neural networks on near term processors. arXiv preprint arXiv:1802.06002 (2018)
- [8] Fogel, D.B.: An introduction to simulated evolutionary optimization. *IEEE transactions on neural networks* **5**(1), 3–14 (1994)
- [9] Freitas, A.A.: A review of evolutionary algorithms for data mining. In: *Data Mining and Knowledge Discovery Handbook*, pp. 371–400. Springer (2009)
- [10] Grimsley, H.R., Economou, S.E., Barnes, E., Mayhall, N.J.: An adaptive variational algorithm for exact molecular simulations on a quantum computer. *Nature communications* **10**(1), 1–9 (2019)
- [11] Jansen, T., Wegener, I.: On the analysis of a dynamic evolutionary algorithm. *Journal of Discrete Algorithms* **4**(1), 181–199 (2006)
- [12] Kandala, A., Mezzacapo, A., Temme, K., Takita, M., Brink, M., Chow, J.M., Gambetta, J.M.: Hardware-efficient variational quantum eigensolver for small molecules and quantum magnets. *Nature* **549**(7671), 242–246 (2017)
- [13] Krylov, G., Lukac, M.: Quantum encoded quantum evolutionary algorithm for the design of quantum circuits. In: *Proceedings of the 16th ACM International Conference on Computing Frontiers*, pp. 220–225 (2019)
- [14] Lahoz-Beltra, R.: Quantum genetic algorithms for computer scientists. *Computers* **5**(4), 24 (2016)
- [15] Ledoux, M.: *The concentration of measure phenomenon*. 89. American Mathematical Soc. (2001)
- [16] McArdle, S., Jones, T., Endo, S., Li, Y., Benjamin, S.C., Yuan, X.: Variational ansatz-based quantum simulation of imaginary time evolution. *npj Quantum Information* **5**(1), 1–6 (2019)
- [17] McClean, J.R., Boixo, S., Smelyanskiy, V.N., Babbush, R., Neven, H.: Barren plateaus in quantum neural network training landscapes. *Nature Communications* (2018). DOI 10.1038/s41467-018-07090-4
- [18] McClean, J.R., Romero, J., Babbush, R., Aspuru-Guzik, A.: The theory of variational hybrid quantum-classical algorithms. *New Journal of Physics* (2016). DOI 10.1088/1367-2630/18/2/023023
- [19] Mücke, S., Piatkowski, N., Morik, K.: Hardware acceleration of machine learning beyond linear algebra. In: *Joint European Conference on Machine Learning and Knowledge Discovery in Databases*, pp. 342–347. Springer (2019)
- [20] Nielsen, M.A., Chuang, I.L.: *Quantum Computation and Quantum Information* (2010). DOI 10.1017/cbo9780511976667
- [21] Peruzzo, A., McClean, J., Shadbolt, P., Yung, M.H., Zhou, X.Q., Love, P.J., Aspuru-Guzik, A., O’Brien, J.L.: A variational eigenvalue solver on a photonic quantum processor. *Nature communications* (2014)
- [22] Pfeuty, P.: The one-dimensional ising model with a transverse field. *ANNALS of Physics* **57**(1), 79–90 (1970)
- [23] Preskill, J.: Quantum Computing in the NISQ era and beyond. *Quantum* (2018). DOI 10.22331/q-2018-08-06-79
- [24] Rudolph, G.: Convergence of evolutionary algorithms in general search spaces. In: *Proceedings of IEEE international conference on evolutionary computation*, pp. 50–54. IEEE (1996)
- [25] Seeley, J.T., Richard, M.J., Love, P.J.: The bravyi-kitaev transformation for quantum computation of electronic structure. *The Journal of chemical physics* **137**(22), 224109 (2012)

- [26] Sherrington, D., Kirkpatrick, S.: Solvable model of a spin-glass. *Physical review letters* **35**(26), 1792 (1975)
- [27] Sofge, D.A.: Toward a framework for quantum evolutionary computation. In: 2006 IEEE Conference on Cybernetics and Intelligent Systems, pp. 1–6. IEEE (2006)
- [28] Spector, L., Barnum, H., Bernstein, H.J., Swamy, N.: Genetic programming for quantum computers. *Genetic Programming* pp. 365–373 (1998)
- [29] Stanley, K.O., Miikkulainen, R.: Evolving neural networks through augmenting topologies. *Evolutionary Computation* (2002). DOI 10.1162/106365602320169811
- [30] Sung, K.J., Yao, J., Harrigan, M.P., Rubin, N.C., Jiang, Z., Lin, L., Babbush, R., McClean, J.R.: Using models to improve optimizers for variational quantum algorithms (2020)
- [31] Swarczman, D., Civitarese, D., Vellasco, M.: Quantum-inspired neural architecture search. In: 2019 International Joint Conference on Neural Networks (IJCNN), pp. 1–8 (2019). DOI 10.1109/IJCNN.2019.8852453
- [32] Tang, H.L., Shkolnikov, V., Barron, G.S., Grimsley, H.R., Mayhall, N.J., Barnes, E., Economou, S.E.: qubit-adapt-vqe: An adaptive algorithm for constructing hardware-efficient ansatzes on a quantum processor. *arXiv preprint arXiv:1911.10205* (2019)
- [33] Wierichs, D., Gogolin, C., Kastoryano, M.: Avoiding local minima in variational quantum eigensolvers with the natural gradient optimizer (2020)
- [34] Zhang, G.: Quantum-inspired evolutionary algorithms: a survey and empirical study. *Journal of Heuristics* **17**(3), 303–351 (2011)

A Proofs

We postponed the proofs to Propositions 1 and 2 and return to the discussion here. For convenience, we restate the propositions.

Proposition 1. *Given a maximally local Hamiltonian*

$$H = \sum_{i=1}^n \sigma_i^{(z)} \quad (13)$$

in each random-gate-choice event the probability of drawing a useful gate is $\geq \frac{1}{4}$ and the number of generations required for optimization is of order $O(n)$.

Proof. Given a generational algorithm where we draw rotation generators $g \in \mathcal{G} \equiv \{\sigma_i^{(x)}, \sigma_i^{(y)}, \sigma_i^{(z)}, \sigma_i^{(x)}\sigma_j^{(x)}, \sigma_i^{(y)}\sigma_j^{(y)}, \sigma_i^{(z)}\sigma_j^{(z)}\}$ applied to qubit i , we are interested in the ground state to $H = \sum_{i=1}^n \sigma_i^{(z)}$. We call the event of drawing a generator capable of optimization S and the respective probability $\mathbb{P}(S)$. We start with the trivial case $n = 1$ and note that $\langle H \rangle$ is invariant with respect to rotations generated by $\sigma^{(z)}$ or $\sigma_i^{(z)}\sigma_j^{(z)}$, such that

$$\langle \psi | R_z^\dagger(\theta) H R_z(\theta) | \psi \rangle = \langle \psi | H | \psi \rangle \quad (14)$$

since $[H, \sigma^{(z)}]_- = 0$, and we find the upper bound $\mathbb{P}(S) \leq 4/6$. Moreover, we can consider $|\psi\rangle$ as superposition of $\sigma^{(x)}$ eigenstates $|\psi\rangle = \alpha|+\rangle + \beta|-\rangle$ and find generator σ^x to be ineffective iff $|\alpha| = 1$ or $|\beta| = 1$. In this case we have $\mathbb{P}(S) = 2/6$ and naturally maximize the effectiveness of $\sigma^{(y)}$. The generalization to n qubits is trivially linear as $|\mathcal{G}| = 6n$. \square

We next consider the second proposition.

Proposition 2. *Let $|\psi_0\rangle$ be the n -qubit ground state to a non-local Hamiltonian defined by*

$$|\psi_0\rangle = \sum_{x \in \{0,1\}^n} a_x |x\rangle \quad (15)$$

with 2^n independent amplitudes a_x . Our algorithm requires $O(2^n)$ operations to find $|\psi_0\rangle$.

Proof. (sketch) In their seminal work [5] the authors discuss for an $(m + 1)$ -qubit system the composition of operations controlled by m qubits. The authors provide proof for an exponentially long circuit requirement for (m) -qubit control in Lemma 7.1. Such operations are composed by having a local unitary

$$U = \begin{pmatrix} u_{00} & u_{01} \\ u_{10} & u_{11} \end{pmatrix} \quad (16)$$

acting on qubit $m + 1$ controlled by qubits $i \leq m$, an operation denoted $\wedge_m(U)$. The authors show that such gates can be composed of $2^m - 1$ gates of class $\wedge_1(U)$ and $\wedge_1^\dagger(U)$, referring to operations controlled by single qubits.

The independence in a_x requires that exclusively operations as in Equation (16) can prepare $|\psi_0\rangle$. The elements of \mathcal{G} have maximal order $\wedge_1(U)$ and therefore have to be ordered in an exponentially long sequence, to prepare the desired ground state. Since we have a stringent upper bound of number of gates added per generation, this leads to an exponential runtime. \square